



ELSEVIER

Journal of Power Sources 95 (2001) 68–78

JOURNAL OF
**POWER
SOURCES**

www.elsevier.com/locate/jpowersour

Advanced bipolar lead–acid battery for hybrid electric vehicles

Michel Saakes^{a,*}, Christian Kleijnen^a, Dick Schmal^a, Peter ten Have^b

^aTNO-Energy, Environment and Process Innovation, Laan van Westenenk 501, P.O. Box 342, 7300 AH Apeldoorn, The Netherlands

^bCenturion Accumulatoren BV, Molensingel 17, 5912 AC Venlo, The Netherlands

Abstract

A large size 80 V bipolar lead acid battery was constructed and tested successfully with a drive cycle especially developed for a HEV. The bipolar battery was made using the bipolar plate developed at TNO and an optimised paste developed by Centurion. An empirical model was derived for calculating the Ragone plot from the results from a small size 12 V bipolar lead–acid battery. This resulted in a specific power of 340 W/kg for the 80 V module. The Ragone plot was calculated at $t = 5$ and $t = 10$ s after the discharge started for current densities varying from 0.02 to 1.2 A/cm². A further development of the bipolar lead–acid battery will result in a specific power of 500 W/kg or more. From the economic analysis we estimate that the price of this high power battery will be in the order of 500 US\$/kWh. This price is substantially lower than for comparable high power battery systems. This makes it an acceptable candidate future for HEV. © 2001 Elsevier Science B.V. All rights reserved.

Keywords: Lead–acid; Bipolar; Hybrid electric; Vehicles; Batteries

1. Introduction

The on-going competition of more fuel economic cars has led to the introduction of the first hybrid electric vehicles (HEV), for example, Toyota (Prius) and Honda (Insight). These very fuel economic cars make use of a high power battery, which stores the energy during braking and delivers the power for acceleration. This battery does not need to be charged separately since it is charged during driving. Recently, Honda's Insight has set a new fuel economy record of 103 miles per gallon.¹ The battery packs, sometimes referred as power packs, are high power nickel metal hydride NiMH batteries. These batteries have a very high specific power value of at least 500 W/kg. The price of these battery packs, however, puts a serious limitation towards the large-scale introduction of these HEV. This relatively high price is due to the low production volumes of the high power NiMH batteries and the relative high price of the basic materials like Ni. In order to lower this price of the power packs, alternatives are investigated. One such alternative is the bipolar lead–acid battery which in principle can be produced at low cost, since mass production is common practice for lead–acid batteries, and also because in principle this battery type is able to give high specific power values as well. Therefore, at TNO, investigations started more than 5 years

ago to explore the possibilities of the bipolar lead–acid battery for HEV applications. In recent publications [1–4] we have demonstrated that the bipolar lead acid battery has potential advantages. This was accomplished by the introduction of TNO of an innovative low weight bipolar plate (patent pending) and an appropriate sealing method. The construction of an 80 V demonstration module, with single cell thickness of approximately 6 mm, resulted in a specific peak power of 250 W/kg [4,5]. This relative low value is due to the use of conventional lead grids, high weight end plates for the construction and a cell thickness of 6 mm.

In order to optimise the specifications of the bipolar lead–acid battery, we performed a 2-year R&D programme in cooperation with a Dutch battery manufacturer. Factors taken into account in this programme, were the development of a special paste for high power applications, the development of a much thinner single cell using newly developed grids and a much thinner plate and the development of an optimised battery management system and cooling system.

The description of these new ideas as well as testing results of a newly built 80 V module incorporating these ideas will be presented. Also, an economic analysis will be given in order to estimate the price of the bipolar lead–acid battery.

2. Experimental part

An 80 V and a 12 V demonstration bipolar lead battery module was built using a newly developed paste for high

* Corresponding author.

E-mail address: m.saakes@mep.tno.nl (M. Saakes).

¹ www.intertechusa.com/energy/eneews/1/news6.htm

current densities. This paste, developed by Centurion Accumulatoren BV, was especially developed for HEV applications and was tested at TNO first in small size 2 V laboratory cells. This paste uses a specially developed hollow C-fiber, which enables the use of high currents even at a low state of charge (SOC).

2.1. 80 V module

The new 80 V module is a complete re-design of the first 80 V module built and tested at TNO in 1998 [4,5]. The reason for this was the use of a much thinner single cell design of approximately 3.4 mm in the second 80 V module compared with 5.8 mm used in the first 80 V module, the use of different plate areas of the positive and negative plate (compensating the difference in capacity), the use of a new construction connecting the spacers with the end-plates and the connection of the individual cells with computer-controlled single cell charge/discharge equipment (home built). The negative plate area was 537 cm² while the positive plate area was 607 cm². The average plate thickness 1.1 mm for the negative plate and 1.3 mm for the positive plate using specially developed gravity cast low antimony (1.6%) grids. An absorptive glass mat (AGM) separator was used as separator.

The bipolar plate thickness was lowered from 0.8 (first 80 V module) to 0.4 mm for the second 80 V module. Because of the lowering of the cell thickness, the glue used for the sealing had to be re-formulated resulting in a specially adapted composition. The internal temperature of the individual cells was measured individually using Pt-100 thermo-resistors put into the cells after sealing the cells. Filling of the cells was done after sealing using 1.28 g/cm³ sulphuric acid solution. The end plates and a cooling plate in the middle of the battery were cooled with deionised water. The end plates were protected with the same materials as used for the bipolar plates. All cycling and HEV experiments were run on a 40 kW Digatron equipment using the latest BTS-600 software. For measuring eight different temperature signals and 40 individual cell potentials, a 48-channel data logger was connected with the bus of the Digatron. In this data logger, each channel had its own AD-converter. The total time for measuring all 48 channels was less than 200 ms enabling a very fast disconnection of the module in case of an alarm signal (e.g. too high temperature or too low or high cell voltage).

HEV drive cycles were run using the latest drive cycles provided by the TNO automotive as developed for a TNO project in which a hybrid vehicle is designed and constructed (P2010). The 80 V module was discharged till 60% SOC before HEV drive cycles were run. All measurements were run at room temperature. The temperature of the battery never exceeded 50°C (high temperature limit) because of the cooling system installed. The individual cell voltages never dropped below 0.5 V/cell (an alarm was generated if one of the 40 cells dropped below 0.5 V automatically switching of

the module). The total voltage of the module was not allowed to drop below 50 V. If the discharge voltage dropped to 60 V, the discharge current was automatically decreased.

2.2. 12 V module

The 12 V module was constructed with small size cells. The pasted plate area was 42 cm² for the negative plate and 56 cm² for the positive plate. The cell thickness was equal to that in the 80 V bipolar module as well as the compression used for the AGM. All single cells were protected during discharge at a minimum voltage of 0.5 V/cell. The end plates, made from aluminium, were connected to a 30 V 100 A galvanostat for measurements. All data were recorded at room temperature. This module was used for determining the rate capability and the power behaviour. From these data the Peukert curve was calculated. For this 12 V module a new type of sealing was introduced which required no longer the use of glue used for the first and second 80 V modules. In this way a very fast proto-typing has become feasible for the bipolar lead-acid battery.

3. Specifications

For the construction of the 80 V prototype, the following main requirements for the HEV were used as a guide.

- Discharge power 50 kW (30 s).
- Charge power 40 kW (30 s).
- Nominal voltage 336 V.
- Maximum weight 150 kg.
- Defined drive cycle translated in a power versus time profile.

The nominal voltage of 336 V is because this voltage can be easily built up using modules of 12 V (28 modules), 24 V (14 modules), 42 V (8 modules) and 84 V (4 modules). The second 80 V module was tested in two ways: as a module of 80 V and as a module of 42 V using the internal cooling plate as an end plate. In case of the 80 V module, results could be directly compared with the first 80 V module. In case of the 42 V section, results can be directly related to the 336 V battery by multiplying the results with a factor 8.

The required power versus time profile is given for two different drive cycles (version 1998 and 1999) as seen in Figs. 1 and 2. The second prototype is shown in Fig. 3 before the cells were filled with acid.

4. Results 80 V module

The 80 V module was tested using hybrid drive cycles from 1998 and 1999. A 42 V section was also tested with high power pulses. An electronic load, developed and built by TNO Prins Maurits Laboratory, was used to test the 42 V section with high current pulses till 550 A.

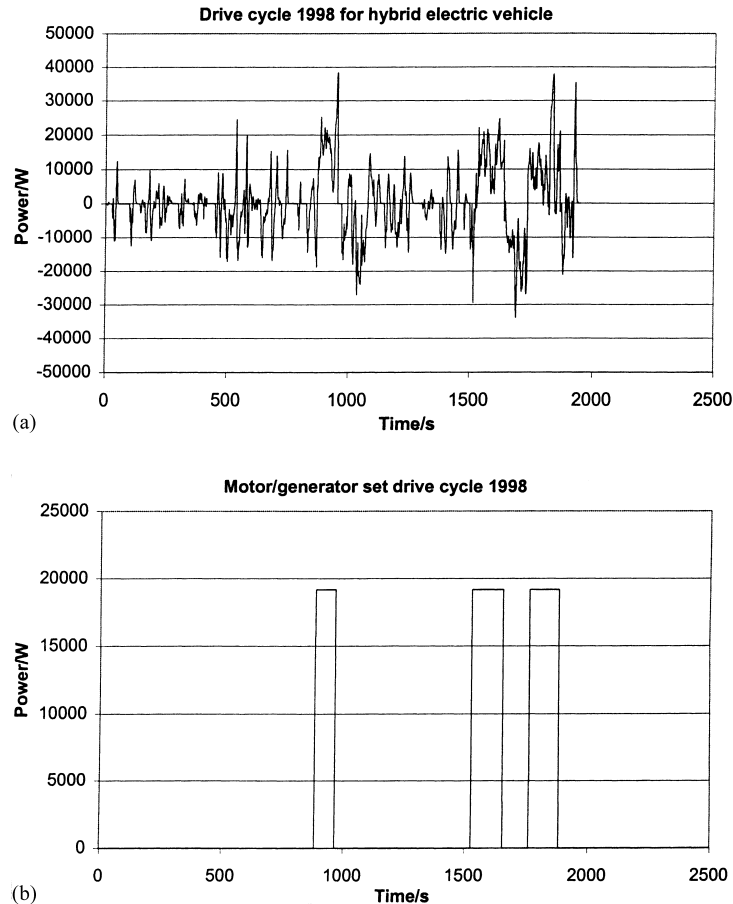


Fig. 1. (a) Drive cycle 1998 for hybrid electric vehicle (HEV); (b) motor/generator set for drive cycle 1998.

In Fig. 4a–e the results for the drive cycle test (version 1999; one-fourth of the total power profile) are shown for the 80 V module for respectively the voltage (V), current (A), power (W), capacity (A h) and energy (W h).

From Fig. 4a–c we conclude that the module is able to deliver the required power profile without exceeding the under limit of 50 V while running the power profile. The discharge current has a maximum of about 125 A. This is equal to a discharge current density of 0.23 A/cm^2 . This discharge current density equals the values obtained for SLI batteries during starting. The bipolar battery is able to deliver during a prolonged time this very high current density.

From Fig. 4d we conclude that the battery is gradually discharged during the drive cycle. The capacity is lowered with a further 2 A h during the drive cycle. The lowering of the capacity can be due to the fact that the acceptance of charge is limited by the over voltage protection of 100 V set for the 80 V module. This is due to the SOC at which the battery is operated. A better charge acceptance is obtained at a lower SOC. The SOC used for starting the drive cycle was 60%. Probably this has to be lowered somewhat.

If we compare the results of the new 80 V module with the results obtained before with the first 80 V module [4,5] with a weight of 75 kg (tested successfully till one-fifth of a

hybrid drive cycle 1998) we conclude that the new module not only has less weight (65 kg) but also performs better (tested successfully with one-fourth of a hybrid drive cycle 1998). The total mass required for four modules of 80 V (second prototype) equals 260 kg. This is a factor 1.7 higher than required.

For the first 80 V prototype this was a factor 2.5 times higher meaning that we have improved the specifications with a factor 1.5. In Fig. 5a–e the results for the drive cycle test (version 1998; one-fourth of the total power profile) are shown for the 80 V module, respectively, for the voltage (V), current (A), power (W), capacity (A h) and energy (W h).

From Fig. 5a–c we conclude that the voltage of the 80 V module never drops below 60 V. The charge voltage is limited to 100 V. Due to this limitation, the charging power has to be limited as well as the charging current. However, these limitations are not seriously affecting the required profile.

From Fig. 5d–e we conclude that the SOC is lowered less than for the 1999 drive cycle version. For the 1998 drive cycle the capacity is lowered about 0.7 A h while for the 1999 drive cycle the capacity is lowered about 1.8 A h.

The results obtained for the new 80 V module show that the bipolar lead–acid battery is able to perform the required

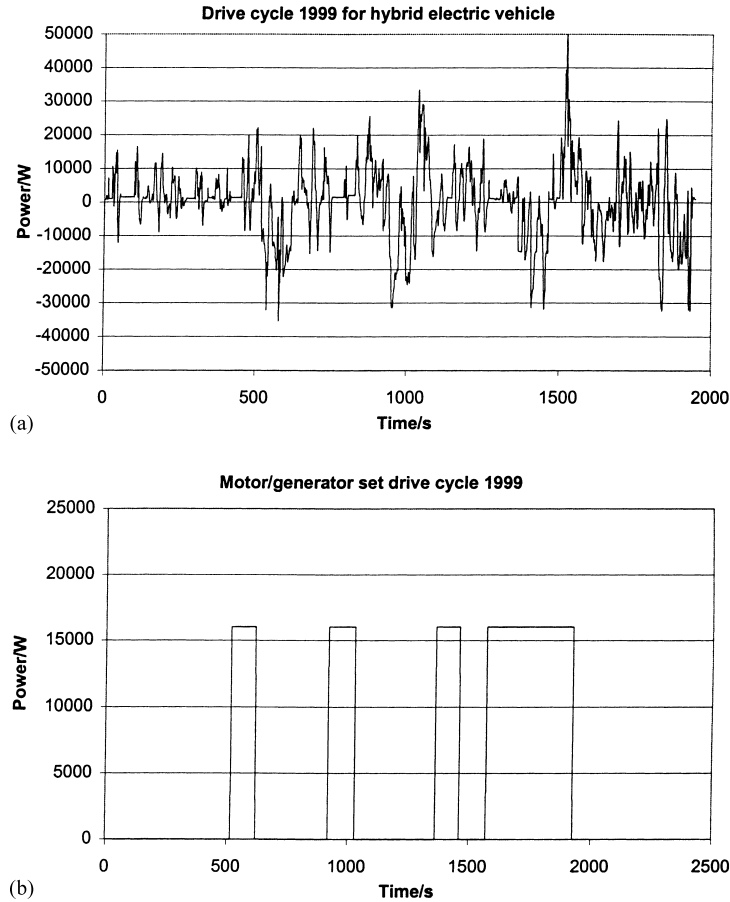


Fig. 2. (a) Newly developed drive cycle (1999) for hybrid electric vehicle (HEV); (b) motor/generator set for drive cycle 1999.

drive cycle. However, the application of the bipolar lead acid battery is practically limited at the moment due to the relatively high weight of the module due to several trivial reasons.

- The weight of the grids is too high. In the bipolar construction a low-weight grid is possible instead of the conventional starter battery grid because the current direction is perpendicular to the plate surface. There is no

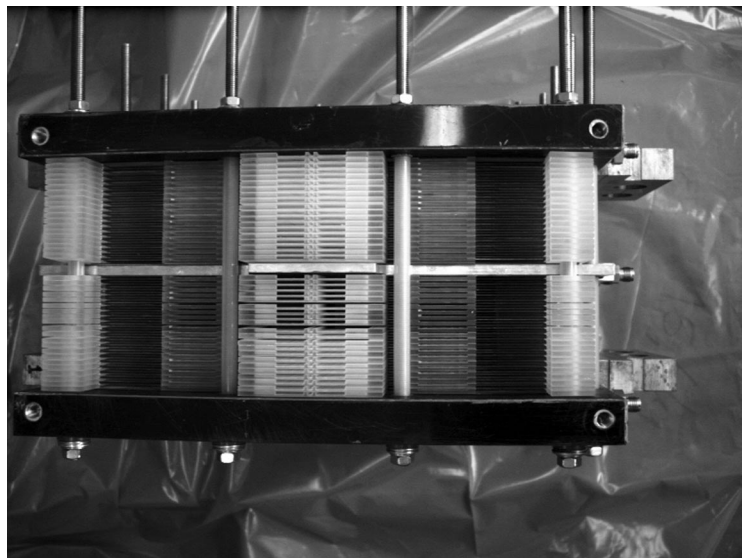


Fig. 3. Photograph of second 80 V 8 A h (C/4) bipolar lead–acid battery module. The weight of this module was 65 kg excluding the internal cooling plate.

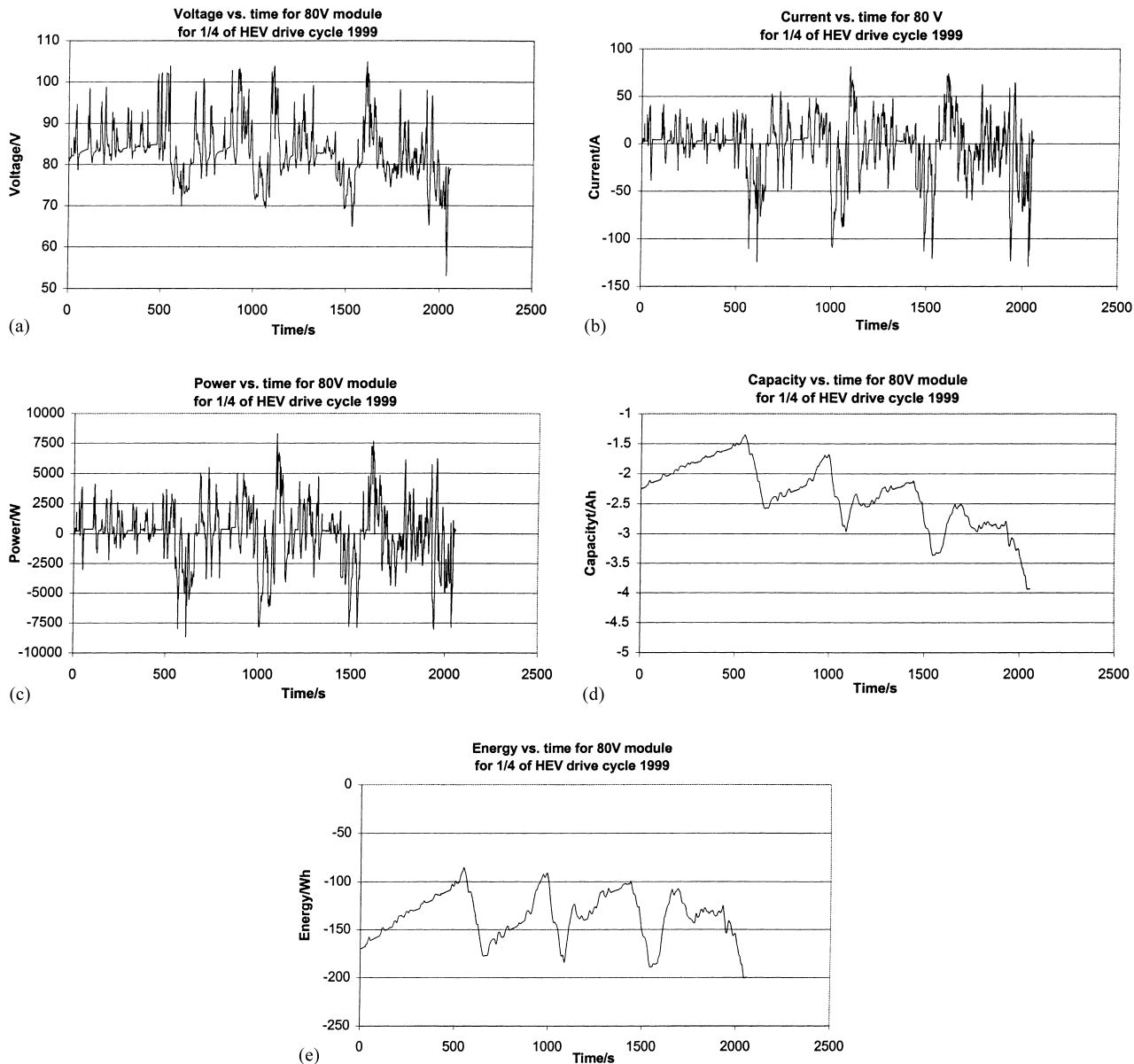


Fig. 4. (a) Voltage (V) vs. time (s) for 80 V module for a one-fourth of a HEV drive cycle (version 1999); (b) current (A) vs. time (s) for 80 V module for a one-fourth of a HEV drive cycle (version 1999); (c) power (W) vs. time (s) for 80 V module for a one-fourth of a HEV drive cycle (version 1999); (d) capacity (A h) vs. time (s) for 80 V module for a one-fourth of a HEV drive cycle (version 1999); (e) energy (W h) vs. time (s) for 80 V module for a one-fourth of a HEV drive cycle (version 1999).

need to carry all current to one tab in a bipolar configuration. The use of lead-plated plastic grids is, therefore, under investigation at TNO.

- The end plates were relatively heavy to the construction used. This can be changed, however, by using a new concept with a plastic casing for keeping single cells together while using thin metal end plate as current collector.
- The sealing, done with special developed glue, requires an adapted spacer construction. Both weight of the glue, as well weight of the spacer, can be lowered by introducing a new sealing concept integrated with the spacer.

If the new developments indicated here will be introduced, we can calculate that the specific power of the bipolar lead–acid battery can be increased to 500 W/kg or more. Especially using low weight pasted grids as well an integral concept for the sealing and single cell design will contribute largely to this improvement.

The pulse power behaviour was tested using the 42 V section of the 80 V bipolar battery by connecting one current collector with the internal cooling plate and one with the end-plate.

Tests were run with 5 kW pulses of 10 s each. In Fig. 6a–c the results are shown. If we calculate this for a 336 V module, the peak power equals 40 kW.

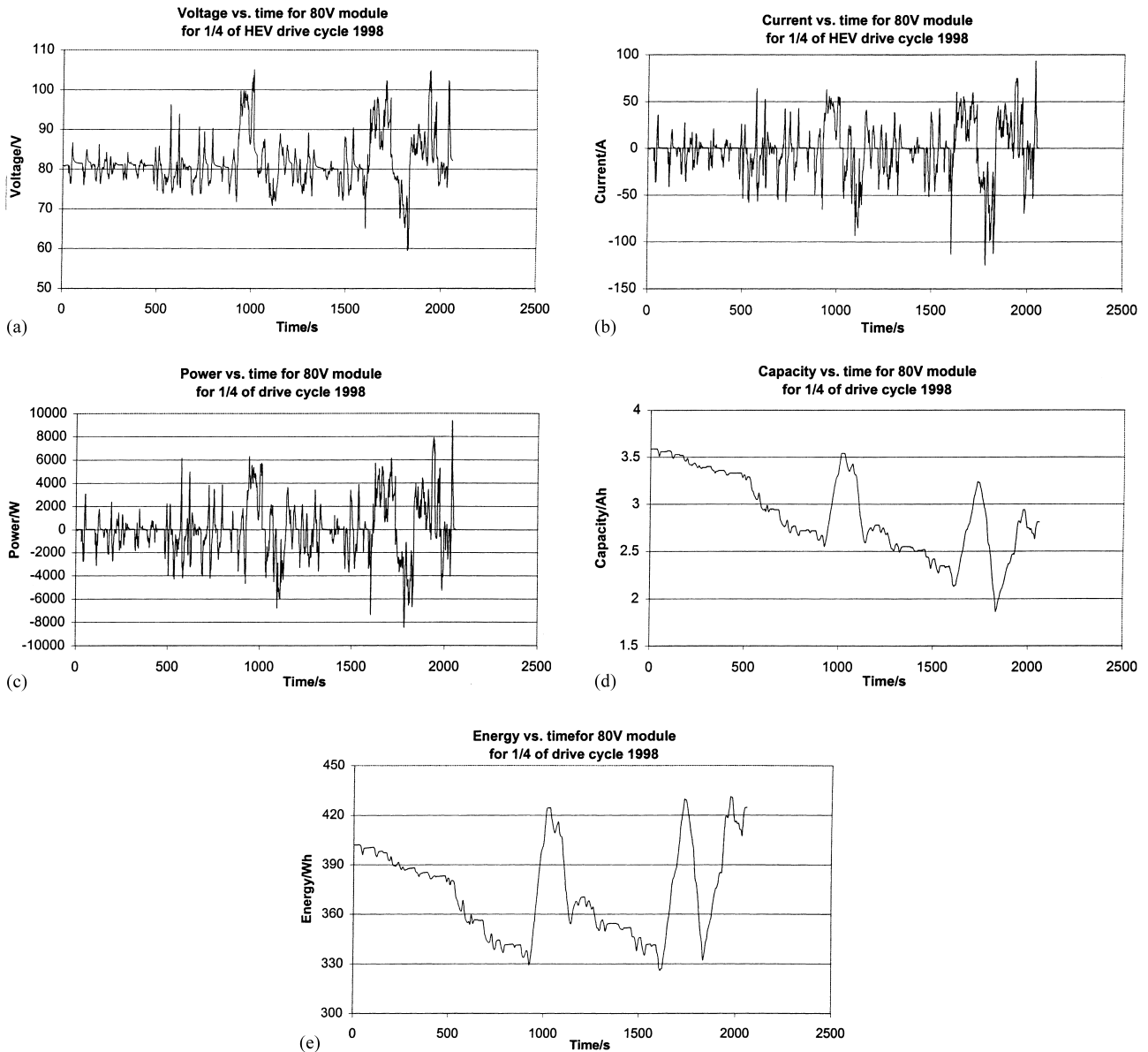


Fig. 5. (a) Voltage (V) vs. time (s) for 80 V module for a one-fourth of a HEV drive cycle (version 1998); (b) current (A) vs. time (s) for 80 V module for a one-fourth of a HEV drive cycle (version 1998); (c) power (W) vs. time (s) for 80 V module for a one-fourth of a HEV drive cycle (version 1998); (d) capacity (A h) vs. time (s) for 80 V module for a one-fourth of a HEV drive cycle (version 1998); (e) energy (W h) vs. time (s) for 80 V module for a one-fourth of a HEV drive cycle (version 1998).

From Fig. 6a we conclude that the voltage drops to about 34 V equal to 1.62 V/cell. From Fig. 6b it is shown that the discharge current is about 140 A. This means that the discharge current density is 0.26 A/cm². This value is typical for the discharge current density for a SLI battery during starting. From Fig. 6c we conclude that the required profile of 5 kW is perfectly performed by the 42 V section.

Besides these pulsed power peaks, we also performed how the 42 V section behaved at 9 kW. Therefore, we tested two peaks of 4 s each. This test was run successfully. The discharge current now reached 300 A. The discharge current density is 0.56 A/cm². Such a high discharge current density cannot be obtained using conventional SLI batteries. The

voltage dropped till 30 V. This means an average discharge voltage of 1.43 V/cell.

From the successfully performed high power peaks we conclude that the bipolar lead battery is not only able to perform HEV drive cycles but also high power peaks for acceleration purposes.

5. Results 12 V module

In order to model the bipolar lead–acid battery, a 12 V bipolar lead–acid battery was built using the pasted plates and compression as used for the 80 V battery. In order to

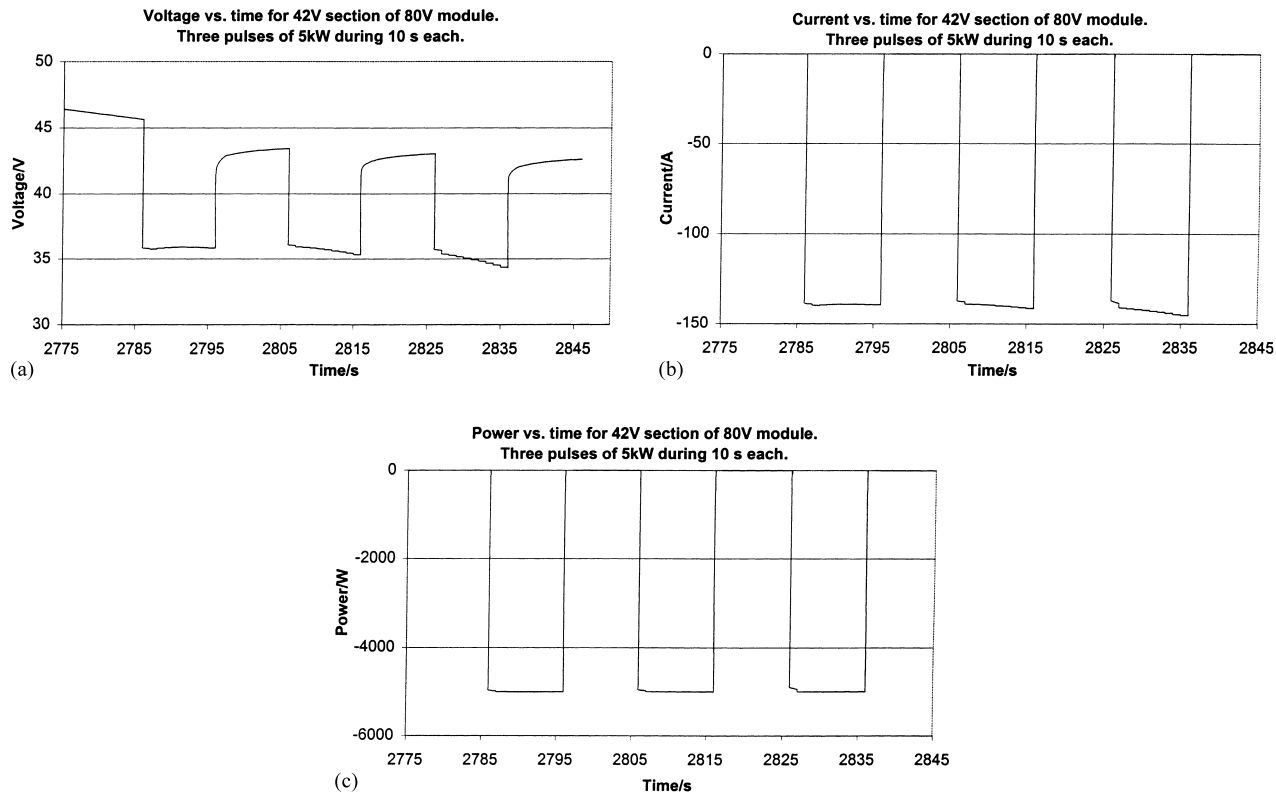


Fig. 6. (a) Voltage (V) vs. time (s) for 42 V section of 80 V module. Test was done using three pulses of 5 kW; (b) current (A) vs. time (s) for 42 V section of 80 V module. Test was done using three pulses of 5 kW; (c) power (W) vs. time (s) for 42 V section of 80 V module. Test was done using three pulses of 5 kW.

simplify the construction, we used a new type of sealing without glue. All single cells were individually protected not to fall below 0.5 V/cell during discharge. The results of the 12 V module will be used to model the bipolar lead–acid battery and also to use the results for up-scaling the battery. This is the reason for fitting the results of the 12 V bipolar lead–acid battery to an empirical model in order to be able to calculate the Ragone plot for the up-scaled 80 V battery.

Because only *constant current discharges* of the 12 V bipolar lead–acid battery were measured, it must be emphasised here that the Ragone plot was constructed by making cross-sections of the experimental obtained power and energy plots during discharge at a given time for the same discharge current. For this, both discharge power as well as discharge energy were calculated as a function of the discharge current. The discharge energy was calculated by multiplying the *average discharge voltage* with the total time of discharge till the voltage dropped below the minimum discharge voltage, at a given discharge current (varying from 1 to 60 A for the 12 V battery). The power at a given time (e.g. $t = 10$ s) was calculated by multiplying the discharge voltage at this time ($t = 10$ s) with the constant discharge current.

Because the discharge voltage varies with time during constant current discharge, the discharge power is

essentially a function of time. As explained, the discharge energy corresponds with a complete discharge at a given current.

In case computer controlled discharge equipment is used, the discharge current can be easily adapted in order to keep the discharge power constant by adapting the control voltage of the galvanostat. In our case, however, we used only constant discharge curves.

The 12 V bipolar lead–acid battery was tested at different discharge current densities within the range of 0.02–1.43 A/cm². In Fig. 7 the Peukert plot is given as the logarithm of the discharge current density versus the time of discharge.

From Fig. 7 we conclude that the bipolar lead–acid battery actually performs very well at very high discharge current densities. The discharge current density reaches a value approximately a factor five times higher than for a SLI battery. This is due to the very low internal resistance of the 12 V module. This resistance was as low as 44 mΩ using a HP milliohmmeter (measuring at 1000 Hz).

In order to determine the Ragone plot for the bipolar lead–acid battery, the rate capability was determined by measuring the discharge capacity Q_{disch} as a function of the discharge current I_{disch} . In Fig. 8 Q_{disch} is given versus I_{disch} .

In order to model the bipolar battery, the rate capability was first fitted to a single exponential function. However, this resulted in a very poor fit as a result of the different

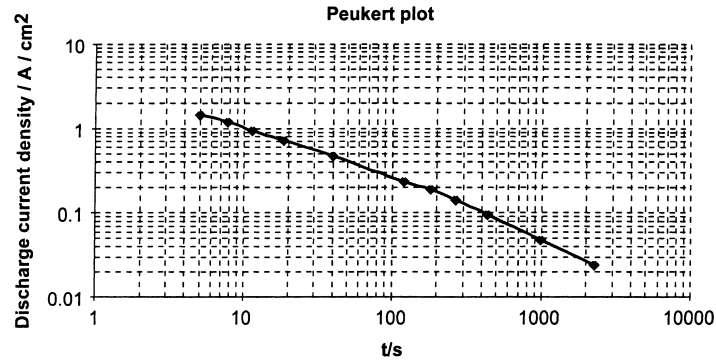


Fig. 7. Peukert plot for a 12 V laboratory scale size bipolar lead–acid battery.

behaviour at low (<0.2 A/cm²) and high (>0.4 A/cm²) current density. Therefore, an attempt was made to fit the discharge capacity with two exponentials given by Eq. (1):

$$Q = \frac{Q_0}{2} \left[e^{-I_{\text{disch}}/a_1} + e^{-I_{\text{disch}}/a_2} \right] \quad (1)$$

with Q_0 equal to the discharge capacity at $\lim(I_{\text{disch}} \rightarrow 0)$ and a_1, a_2 being constants with a dimension equal to Ampere. Fig. 8 shows an excellent fit using Eq. (1) with the parameters equal to $Q_0 = 0.666$ A h, $a_1 = 41.14$ A and $a_2 = 7.29$ A using an optimisation algorithm (OPTDZM) written in HPBasic. From the fitting parameters we conclude that especially at very high current densities the discharge capacity drops at a low rate. The paste was especially developed to perform better at high current densities by using hollow C fibers as additive. These fibers prevent the depletion of acid in the pores of the paste at high discharge current density.

The rate capability is used to calculate the energy by multiplying the discharge capacity with the discharge voltage. For the discharge we will take the average discharge voltage during the various discharge currents. Fig. 9 shows the energy (W h) as a function I_{disch} .

The discharge energy versus discharge current fitted very well using a similar approach for fitting the discharge

capacity versus the discharge current. The fit of the energy E is done using Eq. (2):

$$E = \frac{E_0}{2} \left[e^{-I_{\text{disch}}/b_1} + e^{-I_{\text{disch}}/b_2} \right] \quad (2)$$

The fitting parameters are: $E(\lim I_{\text{disch}} \rightarrow 0) = 7.97$ W h, $b_1 = 29.19$ A and $b_2 = 6.73$ A. Also in this case we find a different behaviour at low and high discharge currents.

Using Eq. (2) we can calculate the Ragone plot once we have the power as a function of the discharge current. We must realise that the power is clearly a function of time since the discharge voltage drops more quickly at higher discharge current densities. The discharge voltage V_{disch} of a single cell is given by Eq. (3):

$$V_{\text{disch}} = V_{\text{OCV}} - I_{\text{disch}} \times R_{\text{ohm}} - \eta_a - \eta_c \quad (3)$$

The open circuit voltage (V_{OCV}) is equal to 2.05 V. The internal voltage drop due to the ohmic resistance is calculated by multiplying I_{disch} with the ohmic resistance R_{ohm} measured using either a milliohm meter or a galvanostatic pulse discharge. The overvoltage η_a and η_c are measured by determining the cell voltage drop as a function of time (both overvoltages are a function of time). Because both η_a and η_c vary with time, we have to be aware that the discharge power, determined at constant current discharge

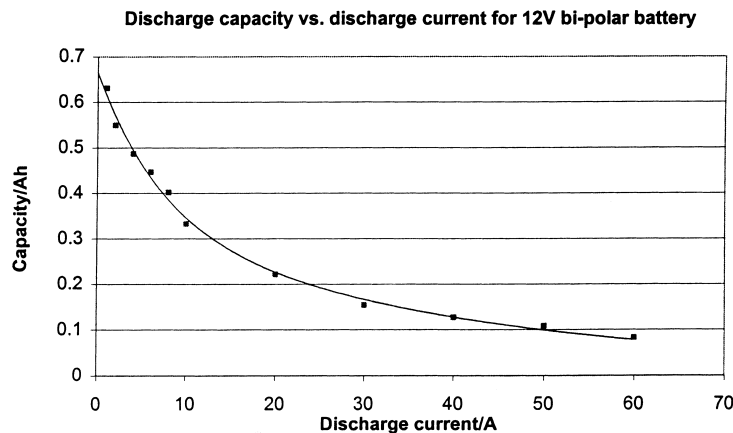


Fig. 8. Q_{disch} vs. I_{disch} for the 12 V bipolar lead–acid battery.

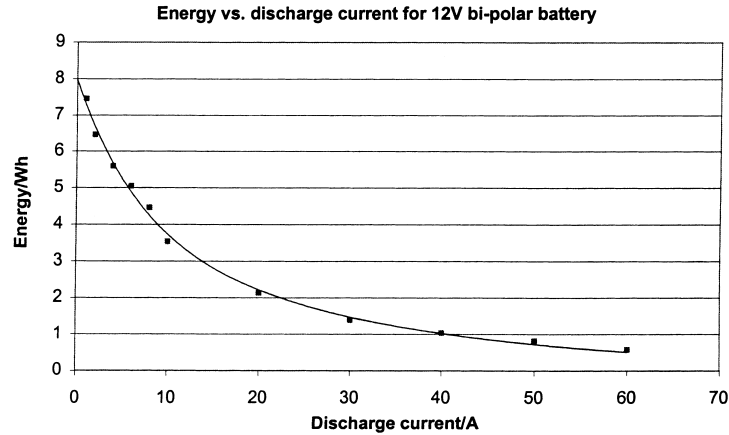


Fig. 9. Discharge energy (W h) as a function of I_{disch} (A) with the fitted curve using Eq. (2).

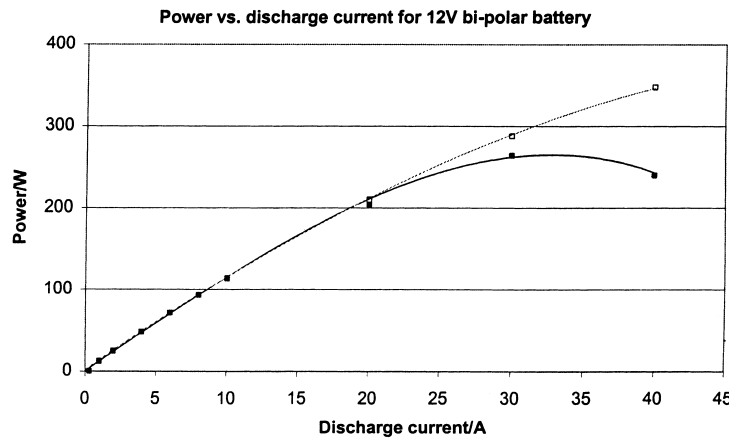


Fig. 10. Discharge power P vs. I_{disch} for $t = 5$ (upper curve) and $t = 10$ s (lower curve) for a 12 V bipolar lead–acid battery.

experiments, is a function of time. For the 12 V bipolar lead–acid battery we measured the discharge power at $t = 5$ and $t = 10$ s after starting the discharge at various currents. We will calculate the Ragone plot for $t = 5$ and $t = 10$ s. The discharge current density was as high as 1.19 A/cm^2 during a total discharge time of 7.8 s.

In Fig. 10 we have plotted the discharge power P versus the discharge current I_{disch} for $t = 5$ and $t = 10$ s.

In order to be able to calculate the Ragone plot for $t = 5$ and $t = 10$ s after starting discharging the battery, it is required to fit P as a function of I_{disch} shown in Fig. 10.

In order to describe P as a function of I_{disch} we fitted P versus I_{disch} using Eq. (4) given by

$$P = b - a_1(I_{\text{disch}} - I_{\text{disch,max}})^2 - a_2(I_{\text{disch}} - I_{\text{disch,max}})^3 \quad (4)$$

where b , obtained by using the boundary condition $P(I_{\text{disch}} = 0) = 0$, is given by Eq. (5)

$$b = I_{\text{disch,max}}^2 (a_1 - a_2 \times I_{\text{disch,max}}) \quad (5)$$

The fitting parameters using Eqs. (4) and (5) are given in Table 1 for $t = 5$ and $t = 10$ s.

Using these parameters obtained for Eqs. (4) and (5) and the parameters for Eq. (2), we are able to calculate the required Ragone plot.

The Ragone plot for the 12 V bipolar lead–acid battery is obtained by plotting P versus E as a function of the discharge current I_{disch} . This is done by calculating numerical values of both P (W) and E (W h) as a function of I_{disch} for $t = 5$ and $t = 10$ s after starting the discharge at various discharge currents.

In Fig. 11 we show the Ragone plot for the 12 V bipolar lead–acid battery. Using Fig. 11 we can perform the up scaling of the battery from 12 to 80 V or any other battery voltage required.

Table 1
Fitting parameters for P as function of I_{disch} for $t = 5$ and $t = 10$ s

a_1 (W/A ²)	a_2 (W/A ³)	$I_{\text{disch,max}}$ (A)
0.3838	0.0042	32.8
0.1325	0.0003	58.7

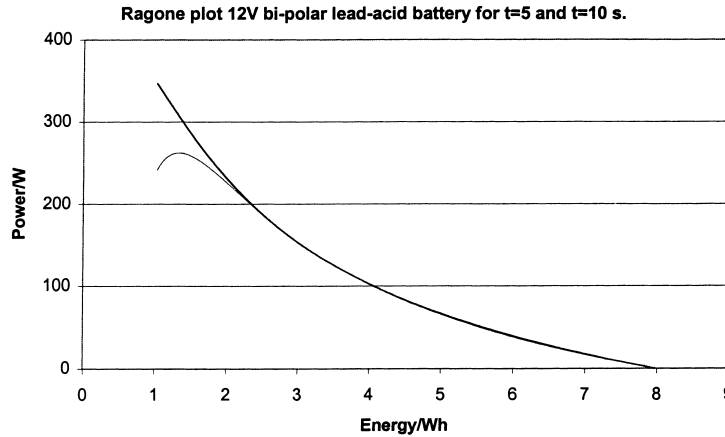


Fig. 11. Ragone plot 12 V bipolar lead–acid battery. This plot was calculated using the average discharge voltage at $t = 5$ and $t = 10$ s and the discharge energy at various constant discharge currents till the voltage dropped till 0.5 V/cell. The maximum occurring in the lower curve is due to the maximum in the power because of the drop in the discharge voltage at very high current densities at $t = 10$ s. This drop is because of depletion of acid. The upper curve gives the power in case this depletion is not yet present (at $t = 5$ s after starting the discharge).

6. Up scaling

The up scaling of the results obtained with the 12 V bipolar lead–acid battery module is done by the following rules

- Multiplying with the ratio of the plate areas.
- Multiplying with the ratio of the voltages.

Comparing the 12 and the 80 V bipolar battery, the ratio of the plate area is equal to 537/42 while the ratio of the voltages is equal to 80/12. The total multiplication factor is, therefore, 85.

In order to express the Ragone plot in terms of the specific energy and the specific power we need to divide the calculated energy and power with the actual mass of the 80 V battery, in our case 65 kg. This weight is still relatively

heavy due to the high weight of the grids and the end plates used. In the near future, the total weight of the battery can be reduced by at least 30% using low weight grids and end plates and a low-weight casing.

Fig. 12 shows the calculated Ragone plot using the experimentally obtained results from the 12 V bipolar lead–acid battery, fitted to Eqs. (2), (4) and (5) and using the multiplication factor of 85 and the weight of 65 kg for the 80 V module.

From Fig. 12, we conclude that the maximum specific power is about 450 W/kg. This value is still too low for application in a HEV since this application required a specific power of at least 500 W/kg. As argued above, improvement of the bipolar lead–acid battery will result in a lowering of the weight with at least 30%. This means that the weight for the 80 V module can be lowered to

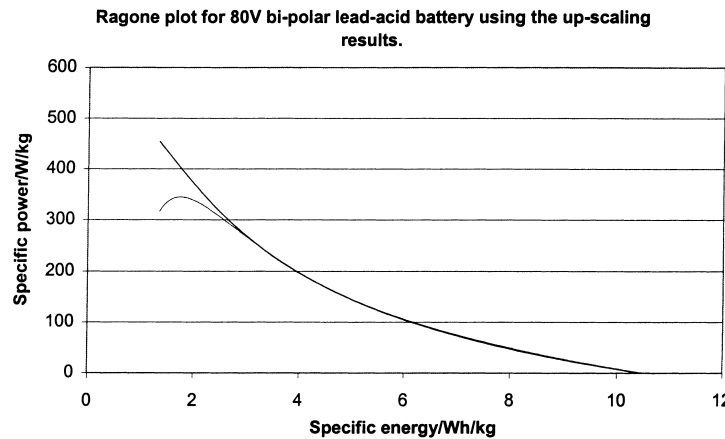


Fig. 12. Ragone plot calculated after the up scaling the results of the 12 V battery to the 80 V module. The power was calculated using the average discharge voltage at $t = 5$ and $t = 10$ s after start of discharge. The discharge energy was calculated at various discharge voltages till the cell voltage dropped below 0.5 V/cell. The upper curve is for $t = 5$ s and the lower curve is for $t = 10$ s. At $t = 10$ s the Ragone plot has a maximum due the strong decrease of the discharge voltage. This is because of the depletion of acid at very high current densities at $t = 10$ s after starting the discharge.

approximately 45 kg. The maximum value of the specific power is then increased to more than 500 W/kg. This is acceptable for HEV applications.

Another point of attention is the specific energy. For a power P to energy E ratio of 25 W/W h (as an example 500 W/kg and 20 W h/kg), the specific energy of the 80 V bipolar lead–acid battery has to increase. At this moment the specific energy is still too low as a consequence of the high weight of the grids and the applied end plates. However, lowering the weight of these parts of the bipolar battery will enable to have a specific energy in the order of 20 W h/kg.

6.1. Short power pulses

As shown in Fig. 12 the specific power is higher for short discharge pulses as demonstrated for $t = 5$ s. This is important in case of true peak demands. For HEV applications, in most cases a typical time for pulse loads or charge pulses will be in the order of 10 s. Very short pulses (1 s or less) are interesting, for example, pulse power applications, e.g. laser pulses. For these very short pulses a bipolar lead–acid battery can deliver a very high specific power because of the very high current densities possible (in the order of 2–4 A/cm²).

We conclude that the bipolar lead–acid battery technology developed at TNO clearly has demonstrated that this battery technology is an acceptable power source for high power applications like HEV. Also for pulse power applications the bipolar lead–acid battery is an attractive candidate. Another advantage of the bipolar lead–acid battery is the low cost of the components as well as the infrastructure available for recycling lead.

Further development programme of TNO is pointing at the use of low weight grids instead of the gravity cast lead grids, a new type of sealing which can be applied much more easy in mass production, a low weight casing and, very important, a battery management system with single cell management and protection. Also the advanced cooling system like already used for the new 80 V module, will

be further developed. Finally, the special paste developed will be further optimised for HEV applications.

7. Economic analysis

From the materials used and the production processes we have analysed the price of the bipolar lead–acid battery for mass production. From this analysis, we have found an estimated price of 500 US\$/kWh in small mass production (25,000 modules per year). For the production costs we have used the general applicable rules for mass production for lead–acid batteries using pick-and-place robots. For the materials, we have used the mass production prices given by the manufacturers of the materials used in the bipolar lead–acid batteries we have constructed.

Acknowledgements

The development described has partly been funded by NOVEM, The Netherlands Agency for Energy and Environment (project no. 245-101-6093). Other funds have been obtained from TNO Automotive and TNO Environment, Energy and Process Innovation and from Centurion Accumulatoren BV. The development could not have been done without prior and parallel funding from TNO Defence Research and the Royal Netherlands Navy for the pulse power application.

References

- [1] M. Saakes, D. Schellevis, D. van Trier, M. Wollersheim, J. Power Sources 67 (1997) 33–41.
- [2] M. Saakes, D. Schmal, R. Pantoflet, in: Proceedings of the 12th International Lead Conference, 22–25 September 1997, Salzburg, Austria.
- [3] M. Saakes, D. Schmal, in: Proceedings of the 6th European Lead–acid Battery Conference, 22–25 September 1998, Prague.
- [4] M. Saakes, E. Kluiters, D. Schmal, S. Mourad, Peter ten Have, J. Power Sources 78 (1999) 199–204.
- [5] D. Schmal, M. Saakes, S. Mourad, Peter ten Have, 32nd ISATA, 14–18 June 1999, Vienna, Austria.